Journal of Superconductivity and Novel Magnetism (2018) 31:3847–3854
https://doi.org/10.1007/s10948-018-4678-8

ORIGINAL PAPER

Study of Critical Current and *n*-Values of 2G HTS Tapes: Their Magnetic Field-Angular Dependence

X. Zhang[1] · Z. Zhong[1] · J. Geng[1] · B. Shen[1] · J. Ma[1] · C. Li[1] · H. Zhang[1] · Q. Dong[1] · T. A. Coombs[1]

Received: 21 March 2018 / Accepted: 29 March 2018 / Published online: 24 April 2018

Abstract

Since many applications of YBCO tapes operate in external magnetic fields, it is necessary to investigate the magneto-angular dependence of critical current and *n*-values in coated conductors. In this paper, five commercial YBCO tapes with different microstructures produced by three different manufacturers are chosen. The selected samples have a width of 2.0, 4.0, 4.8, 6.0 or 12 mm, with copper, brass or stainless steel laminations. The critical current density dependence $J_c(B, \theta)$ and *n*-values characteristics $n(B, \theta)$ of the tapes are comprehensively measured under various magnetic fields and orientations. Afterwards, the obtained experimental data sets are successfully fitted using a novel multi-objective model which considers the material anisotropy. By using this approach, a fitting function $I_c(B, \theta)$ can always be obtained to accurately describe the experimental data, regardless of the fabrication and width differences of the superconducting tapes. Moreover, our experiment shows that when subject to different external magnetic fields, the angular dependence of *n*-values characteristics is directly correlated with the corresponding critical current profiles. Our results are helpful to predict the critical current of electromagnetically interacting 2G HTS wires, thereby improving the design and performance of the devices made from YBCO tapes.

Keywords YBCO tapes · Critical current density · *n*-values · Magnetic field-angular dependence

1 Introduction

Along with the development of high-temperature superconducting (HTS) materials, long lengths of high-quality YBCO-coated conductors are now commercially available [1–4]. YBCO-coated conductors are one of the most promising superconducting materials that can be used in the power system. The most successful HTS devices, including superconducting fault current limiters, power transmission cables and transformers, have shown their superiorities and potentials compared with their conventional alternatives [5, 6]. Moreover, the cost-performance ratio is getting better thanks to the progress in material researches, which facilitates further development of superconducting applications. In addition, the cost of devices can be further reduced by optimizing the layout and also minimizing the quantity of YBCO-coated conductors that is required by an apparatus. This optimization process needs information of the magnetic field-angular dependence of critical current density $J_c(B, \theta)$ [7].

However, since YBCO tapes present complex anisotropy, and this anisotropic field dependence is significantly influenced by the sample preparation methods, the $J_c(B, \theta)$ characteristics of YBCO are hard to be predicted and modelled accurately without measurement [3, 8]. Furthermore, experimental data on the self-field behaviour of the tapes are not adequate for modelling the electrical performance of HTS devices, since the power equipment normally operates under external magnetic fields [9]. Therefore, in order to support modelling of superconducting applications, measuring the magnetic field-angular dependence of YBCO-coated conductors thoroughly is of great importance.

To solve this problem, previously, we have measured the magneto-angular dependence of critical current density of five different YBCO commercial tapes [10]. During the fitting process of these results, the validity of our novel multi-objective model was successfully proved. We have

✉ X. Zhang
xz326@cam.ac.uk

[1] Department of Engineering, University of Cambridge, Cambridge CB3 0FA, UK

shown that a universal description function $I_c(f(B), \theta)$ can be obtained based on the five tested tapes, despite significant differences existing during their fabrication and composition processes.

In this paper, in order to study further the magneto-angular dependence of 2G HTS tapes and test the applicability of our fitting model, we present experimental and numerical outcomes of five different commercial tapes. The tested YBCO-coated conductors have five different widths and three different types of laminations, and are produced by three different manufacturers. The critical current and n-values characteristics of the studied tapes are measured under external magnetic fields with the magnitude changing from 50 mT to 100, 150, 200 and 300 mT. For exploring angular dependence, 90 measurements from -90 to 90° (with an increment of 2°) are taken under each magnetic field for every tape. Afterwards, the fitting model we generalized before is applied to fit the experimental results.

This paper is organized as follows. In Section 2, the experimental setup and the detailed information of the studied YBCO tapes are presented. Afterwards, Section 3 demonstrates the anisotropic field dependence of the critical current of the tapes and the extended Kim model-based fitting process. Then, Section 4 presents the calculation process and analysis of n-values of the samples. Finally, the main conclusions of this paper are summarized in Section 5.

2 Experimental Setup and Measured Samples

A 600-mT electromagnet with a large homogeneous field area (∼ 204 mm pole face diameter) was used for measuring the magnetic field-angular dependence of the critical current of the samples. The YBCO tapes were coaxially fixed under a high-precision rotary stage which had a graduation of 1° and Vernier of 5′. The rotating stage and a mounted sample are shown in Fig. 1. In order to measure the voltage signals, twisted copper wires (Ø 0.4 mm) were soldered on the nameplate side of the YBCO tapes using a low-temperature solder. The solder-flux was chosen according to the manufacturers' suggestions to guarantee better electrical connection. Specifically, zinc chloride flux was selected for tapes with brass and copper laminations, while highly corrosive solder flux was used when soldering stainless steel-laminated tapes.

In order to reduce the contact resistance, all tested samples were set to be 180 mm long, with a contact length of 40 mm at each terminal. Moreover, with high-purity indium covering both ends as cold welding, the contact resistance was reduced to as low as ∼0.5 mΩ for 4-mm tapes and ∼0.15 mΩ for 12-mm tapes at room temperature.

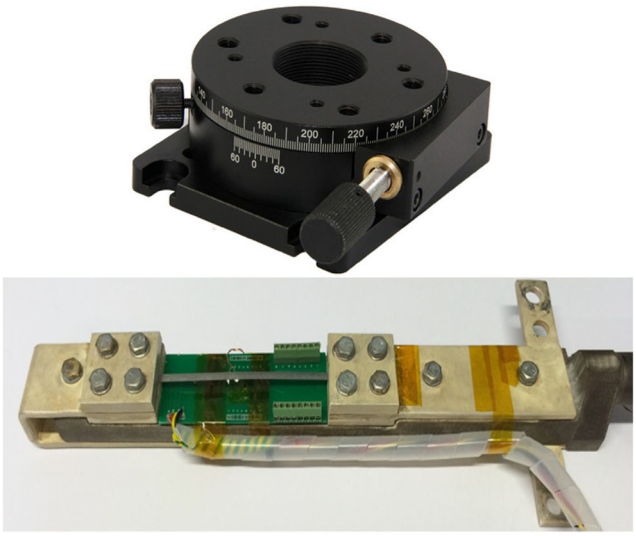

Fig. 1 (Colour online) Photograph of the rotary stage and a mounted YBCO sample

A four-probe method was employed in evaluating I_c, and the voltage criterion V_c was defined as 1×10^{-4} V/m. The transport current was supplied by current source Agilent 6680A, and the signals that were picked up by the voltage taps were monitored by a Keithley 2182A nanometer. The entire experimental system was controlled by a LabVIEW platform. In addition, all the experiments were conducted in liquid nitrogen baths (77 K).

The YBCO tapes we measured were produced by three different manufacturers: SuperPower Inc. (SP), Shanghai Superconductor Technology Co. Ltd. (SHSC) and SuperOx (SO). To be more specific, two types of 2G HTS tapes from SP were tested: surround copper stabilizer tapes of 2 mm width (SCS2050) and 6 mm (SCS6050), respectively. The tapes are made by metal-organic chemical vapour deposition (MOCVD) on an ion beam assisted deposition made MgO template. The YBCO layer of the two tapes is 1 μm thick, and the substrate of both samples is non-magnetic commercial compound Hastelloy C-276, with a thickness of 50 μm. Two 2-μm silver layers made by the sputtering technique are coated outside the YBCO layer and the substrate, providing outstanding electrical contacts [11]. The third and fourth samples come from SHSC, with widths of 4 mm (ST-04-E) and 4.8 mm (ST-05-L), respectively. Both tapes have non-magnetic commercial compound Hastelloy substrate and metal-organic deposited YBCO layer. However, it is worth mentioning that ST-04-E is electroplated with brass, while ST-05-L has a stainless steel lamination [12]. The last sample refers to the 12-mm-wide, 0.12-mm-thick YBCO tape that was manufactured by SuperOx, also called SO-12. This tape has a cold-rolled and electro-polished Hastelloy C-276 substrate with a width

Table 1 Technical parameters of the superconducting wires

2G HTS tapes	Total thickness (mm)	Width (mm)	Critical current (A)	n-value
SCS2050	0.095	2.0	58.8	32.5
SCS6050	0.095	6.0	166.6	31.9
ST-04-E	0.130	4.0	112.0	38.2
ST-05-L	0.350	4.8	175.3	45.1
SO-12	0.120	12.0	301.4	34.4

of 60 μm. The YBCO layer is fabricated by pulsed laser deposition (PLD) over a buffer of heteroepitaxial layers deposited by sputtering on the substrate. Moreover, outside the silver and copper electroplating, the tape is covered by 5-μm-thick surround polyimide coating [13]. Further information about the technical specifications of the five tested tapes is gathered in Table 1.

3 $J_c(B, \theta)$ Dependence of 2G HTS Tapes

3.1 Experimental Result

The variation of critical current I_c along with the applied magnetic field and its orientation is presented in Fig. 2. The magnetic field was always applied in the direction perpendicular to the transport current, which is the maximum Lorentz force configuration. The field angle θ is defined as 0° when the external magnetic field is parallel to the *ab*-plane of HTS tapes, as illustrated in Fig. 2a.

The anisotropic angular-field dependence of YBCO thin films is mainly affected by two factors, first, the effect of the electron mass anisotropy ratio $\gamma^2 = m_c^*/m_{ab}^*$ that was proposed by Blatter et al. [14], i.e., the ratio between the effective mass of the charge carriers along the *c*-axis and the *ab*-plane of the YBCO layer. Microscopic research have shown that, in commercial 2G HTS tapes, only a small fraction of YBCO grains have their *ab*-planes precisely parallel to the tape surface, while the *ab*-planes

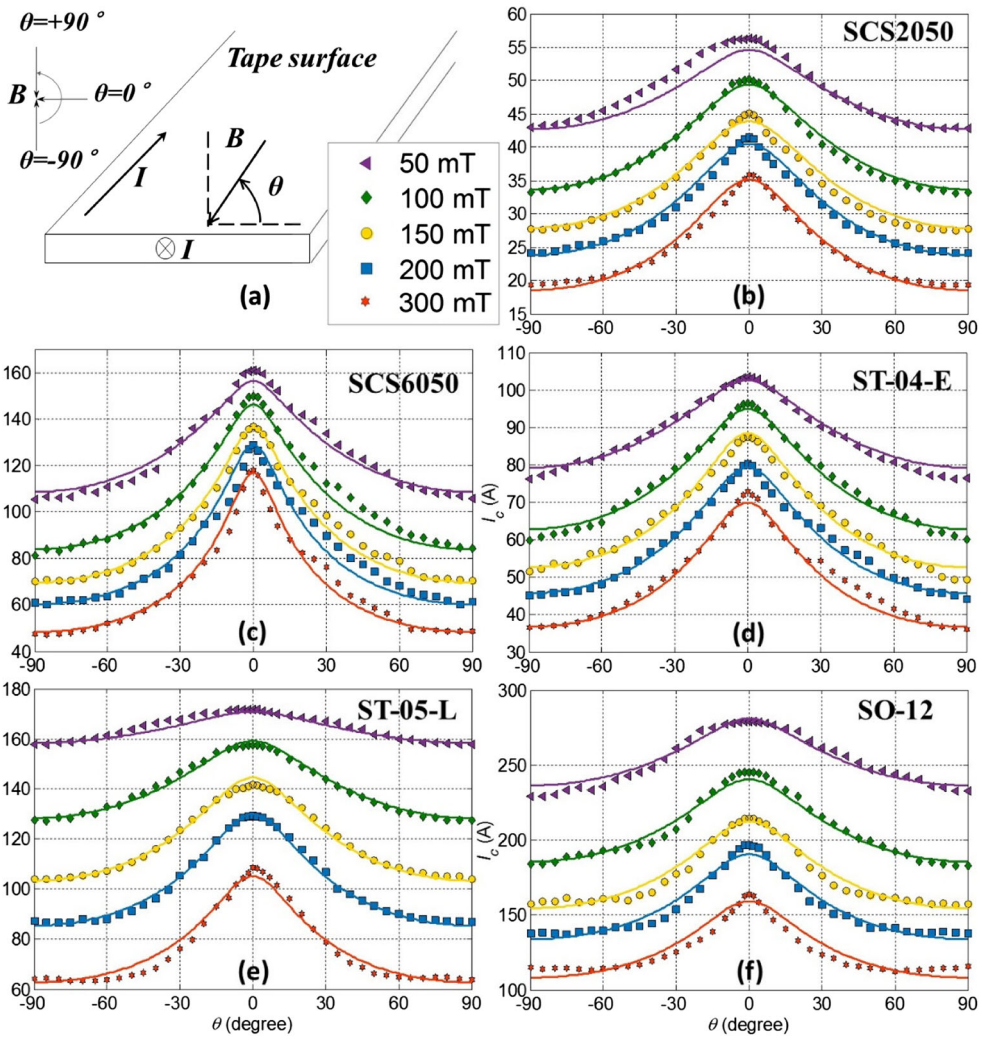

Fig. 2 (Colour online) Magnetic field-angular dependence of measured commercial YBCO tapes: comparison between experimental data (symbols) and fitting curves (solid lines)

of most YBCO grains align imperfectly. Therefore, a peak of critical current appeared when external magnetic field applied parallel to the tape, as can be observed from Fig. 2b–f. Second, intrinsic pinning must be taken into account when vortices are approximately parallel to the *ab*-plane. This is due to the small coherence length along the *c*-axis (ξc) compared with the layer separation ($d \sim 1.2$ nm) in high-Tc superconductors [15]. These two mechanisms are non-linearly combined with each other and may individually become the dominant pinning force at certain field orientations.

It can be seen from Fig. 2 that the variation trends of critical current in samples from different commercial enterprises possess similar qualitative features, suggesting that the same pinning mechanism might be at play. In general, all tapes exhibit noticeable peaks when the external magnetic field is parallel to the film surfaces ($B//ab$). However, it fails to show another peak centred at $B//c$, indicating that the effect of correlated pinning (or intrinsic pinning) is insignificant under moderate magnetic fields. Detailed information about percentage decline of magnetic field critical current ($B = 50$ mT or $B = 300$ mT, $\theta = 0°$ and $\theta = \pm 90°$) relative to self-field critical current in measured YBCO commercial tapes has been calculated and gathered in Table 2.

Specifically, the 6 mm SuperPower sample SCS6050 shows the most significant angular dependence among all measured tapes. Under 300 mT external magnetic field, it experiences the smallest percentage decline 28.7% at $\theta = 0°$ (B $\parallel$ *ab*-plane, B $\perp$ I), while the biggest percentage decline 70.1% shows at $\theta = \pm 90°$ (B $\parallel$ *c*-axis, B $\perp$ I). The strong anisotropic characteristic makes this YBCO sample suitable for applications in which the external field is always parallel to the *ab*-plane of the tape, since relatively a high critical current can still be preserved with an increase of the field density.

Compared with SCS6050, the other SuperPower sample SCS2050 has a smoother descending of I_c when the external field increases: from the self-field critical current 58.8 A reduced by 31.7% at 300 mT/0° and 67.8% at 300 mT/90°, as shown in Fig. 2b. Then, further measurement reveals that, along with changes of angle and intensity of the external magnetic field, the variation trend of critical current profiles of ST-04-E from Shanghai Superconductor is very similar to SCS2050. The differences between the average percentage decline of ST-04-E and SCS2050 are only 3.6% at 50 mT and 2.5% at 300 mT, respectively.

The remaining two YBCO samples, ST-05-L from Shanghai Superconductor and SO-12 from SuperOx, are less sensitive to the angle and density of the external magnetic field, indicating that these two tapes have better in-field performance in moderate fields. Among all measured 2G HTS wires, the one with the lowest magnetic-angular dependence is SO-12, in which the critical current curve is less angular sensitive under high magnetic field, as can be seen from Fig. 2f. With this relatively isotropic property, SO-12 is capable of performing very well when assembled in rotating devices, e.g., superconducting motors, due to its high effective critical current in varying the electromagnetic environment compared with other measured samples.

3.2 Curve Fitting

In our previous work, we have proposed a fitting method that can successfully describe the magneto-angular dependence of critical current in 2G HTS tapes. The equation we derived is an extended version of the Kim model [16], which takes into account the material anisotropy and the flux-creep processes of YBCO samples [10]. Our approach can be generalized as

$$I_c(\theta, B) = I_{c0}\left[1 + \varepsilon_\theta \left(\frac{B}{B_0}\right)^{\alpha}\right]^{-\beta} \tag{1}$$

with

$$\varepsilon_\theta = \sqrt{\gamma^{-2}\sin^2(\theta) + \cos^2(\theta)} \tag{2}$$

In (1), $I_{c0} = I_c(0, \theta)$ represents the self-field critical current, while B is the norm of the magnetic flux density. In addition, B_0 and β are empirical parameters introduced by Kim. The thermally activated flux-creep characteristics of specific samples can be well described by properly adjusting their values. Moreover, we added a variable α into the equation, for making this fitting approach more accurate

Table 2 Percentage decline (P_d) of magnetic field-critical current (50 and 300 mT, and $\pm 90°$) with respect to self-field critical current for the studied 2G HTS tapes

	Width (mm)	I_c (0 mT, 0°) (A)	P_d (50 mT, 0°) (%)	P_d (50 mT, $\pm 90°$) (%)	P_d (300 mT, 0°) (%)	P_d (300 mT, $\pm 90°$) (%)
SCS2050	2.0	58.8	5.1	27.1	31.7	67.8
SCS6050	6.0	166.6	4.2	37.1	28.7	70.1
ST-04-E	4.0	112.0	8.0	31.3	35.7	66.9
ST-05-L	4.8	175.3	3.9	9.2	38.8	64.0
SO-12	12.0	301.4	8.3	24.6	45.5	61.1

and more general. In order to minimize the number of free parameters, the value of α was always fixed to be 1 at the first step of every optimization, and it would only be changed when no preferable fittings could be achieved with this setting. The applied field was also scaled by a function formed based upon the electron mass anisotropy ratio of the material $\gamma^2 = m_c^*/m_{ab}^*$, ranging from 1 to around 25, corresponding to different characteristics between fully isotropic condition and highly anisotropic conductivity of $YBa_2Cu_3O_{7-\delta}$ grains [17].

In order to acquire precise fittings of the YBCO tapes, the self-field critical current I_{c0} in (1) was fixed at values that are listed in Table 1, which left four parameters, B_0, α, β, and γ, to be determined. Then, potential choices for the four parameters were selected empirically [18], to prepare for further calculation. Next, a candidate list of optimal fittings was generated by considering all combinations of the four mentioned parameters, giving $N = N_{B_0} * N_\alpha * N_\beta * N_\gamma$ options in total. Last, for every set of parameters on the candidate list, the mean absolute percentage deviation (MAPD) and the root-mean-square deviation (RMSD) of fitting results with respect to the experimental measurements were calculated based upon the following equations:

$$\delta_{\mathrm{MAPD}} = \frac{1}{N_B N_\theta} \sum_{k=1}^{N_B N_\theta} \frac{|I_{\mathrm{fitting}} - I_{\mathrm{measurement}}|_k}{I_{\mathrm{measurement}}} \tag{3}$$

$$\delta_{\mathrm{RMSD}} = \sqrt{\frac{\sum_{k=1}^{N_B N_\theta} (I_{\mathrm{fitting}} - I_{\mathrm{measurement}})_k^2}{N_B N_\theta}} \tag{4}$$

where $N_B = 5$, representing that we have conducted the J_c (B, θ) experiment in the external magnetic field with five different amplitudes. Moreover, $N_\theta = 90$ stands for the number of experimental orientations in each given field. The standard of being a qualified fitting was set as MAPD smaller than 3%.

The optimal fitting processes revealed that there exist numerous sets of B_0, α, β and γ, which can lead to excellent fittings of the experimental measurements about anisotropic field dependence of YBCO thin films. Taking the 4.0-mm tape ST-04-E for example, we have set $\alpha = 1$ and considered 20 values for each one of the other three parameters, giving 8000 possible combinations in total. The simulation showed that 49 out of the 8000 choices were able to provide fitting results with MAPD lower than 3%. These 49 combinations could be considered as in equally good agreement with the measurements, since YBCO tapes, even those manufactured in the same batch, still possess small statistical variation of physical characteristics [18].

The specific values that we used to fit the in-field angular dependence of ST-04-E (see Fig. 2d) were $B_0 = 80.83$ mT, $\alpha = 1$, $\beta = 0.72$ and $\gamma^2 = 4.35$. The corresponding MAPD and RMSD in this case were, as determined from calculations, 1.75% and 1.48, respectively. Using the same method, for the tape SCS6050 (Fig. 2c), it was found that 83 out of 8000 parameter combinations could lead to precise fitting curves (MAPD within 3%). The lowest MAPD and RMSD in this case were 2.30% and 3.06, which were generated by the following data set: $B_0 = 56.04$ mT, $\alpha = 1$, $\beta = 0.67$ and $\gamma^2 = 7.69$.

Setting $\alpha = 1$ prior to the optimization is suitable for ST-04-E and SCS6050. However, when the studied tapes express more complicated anisotropy of critical current properties, the tolerance requirement between the optimization results and experimental observations can no longer be accomplished: e.g., for the 2.0-mm tape SCS2050, the lowest MAPD and RMSD that can be achieved with $\alpha = 1$ are 5.37% and 3.19, which means the peaks of current curves are distorted by more than 10%.

In order to achieve desirable accuracy and maintain the least number of fitting parameters, the value of α will have to be varied to provide accurate estimations. With an alterable α in the optimizing procedure, the MAPD and RMSD of SCS2050 were substantially reduced to 1.21% and 0.77, respectively. The specific values of the parameters used to obtain fittings shown in Fig. 2b are $B_0 = 58.27$ mT, $\alpha = 1.29$, $\beta = 0.50$ and $\gamma^2 = 4.76$. In the same way, accurate expressions for the $J(B, \theta)$ dependence of the remaining two YBCO samples were achieved as well. For the stainless-steel-laminated tape that was manufactured by Shanghai Superconductor, ST-05-L, minimization showed that with $B_0 = 100.38$ mT, $\alpha = 1.98$, $\beta = 0.45$ and $\gamma^2 = 4.17$, the MAPD and RMSD can be as low as 1.06% and 1.47, respectively (Fig. 2e). In addition, optimal fitting parameters of the 12-mm-wide sample SO-12 were proved to be $B_0 = 53.26$ mT, $\alpha = 1.59$, $\beta = 0.36$ and $\gamma^2 = 3.34$. The corresponding MAPD and RMSD of this fitting are 1.88% and 4.01.

The explorations of $J(B, \theta)$ of all measured commercial tapes were successfully finished. The results above convincingly demonstrated the universality of our numerical approach, since in this paper the YBCO samples we studied were completely different from the samples we used in our previous research. The optimized fitting parameters and precision information of each 2G HTS tape are listed in Table 3.

4 In-Field Angular Dependence of *n*-Value Characteristics

During processes of measuring critical current under different angles and field conditions, for each data point that was plotted in Fig. 2, we have correspondingly stored a unique I-V curve, which contains detailed information about the transition from the superconducting state to

Table 3 Optimal fitting parameters of the tapes and corresponding precision information

2G HTS tapes	I_{c0} (A)	B_0 (mT)	α	β	γ^2	MAPD	RMSD
SCS2050	58.81	58.27	1.29	0.5	4.76	1.21%	0.77
SCS6050	166.55	56.04	1	0.67	7.69	2.30%	3.06
ST-04-E	112.02	80.83	1	0.72	4.35	1.75%	1.48
ST-05-L	175.25	100.38	1.98	0.45	4.17	1.06%	1.47
SO-12	301.42	53.26	1.59	0.36	3.34	1.88%	4.01

the dissipative state. Based on these data, the n-values characteristics in studied YBCO tapes can be calculated: by taking the logarithm for both sides of the E-J power law, it can be derived that

$$\log\left(\frac{V}{V_c}\right) = n * \log\left(\frac{I}{I_c}\right) \tag{5}$$

Thus, n-values can be extracted from the linear fit to $\log(V/V_c)$ vs. $\log(I/I_c)$. By using (5), we have calculated and then plotted the magnetic field-angular dependence of n-values in measured samples, as shown in Fig. 3. During the process of linear curve fitting, a certain level of uncertainty was introduced, which led to visible fluctuation in n-values. However, the overall tendency should be unaffected.

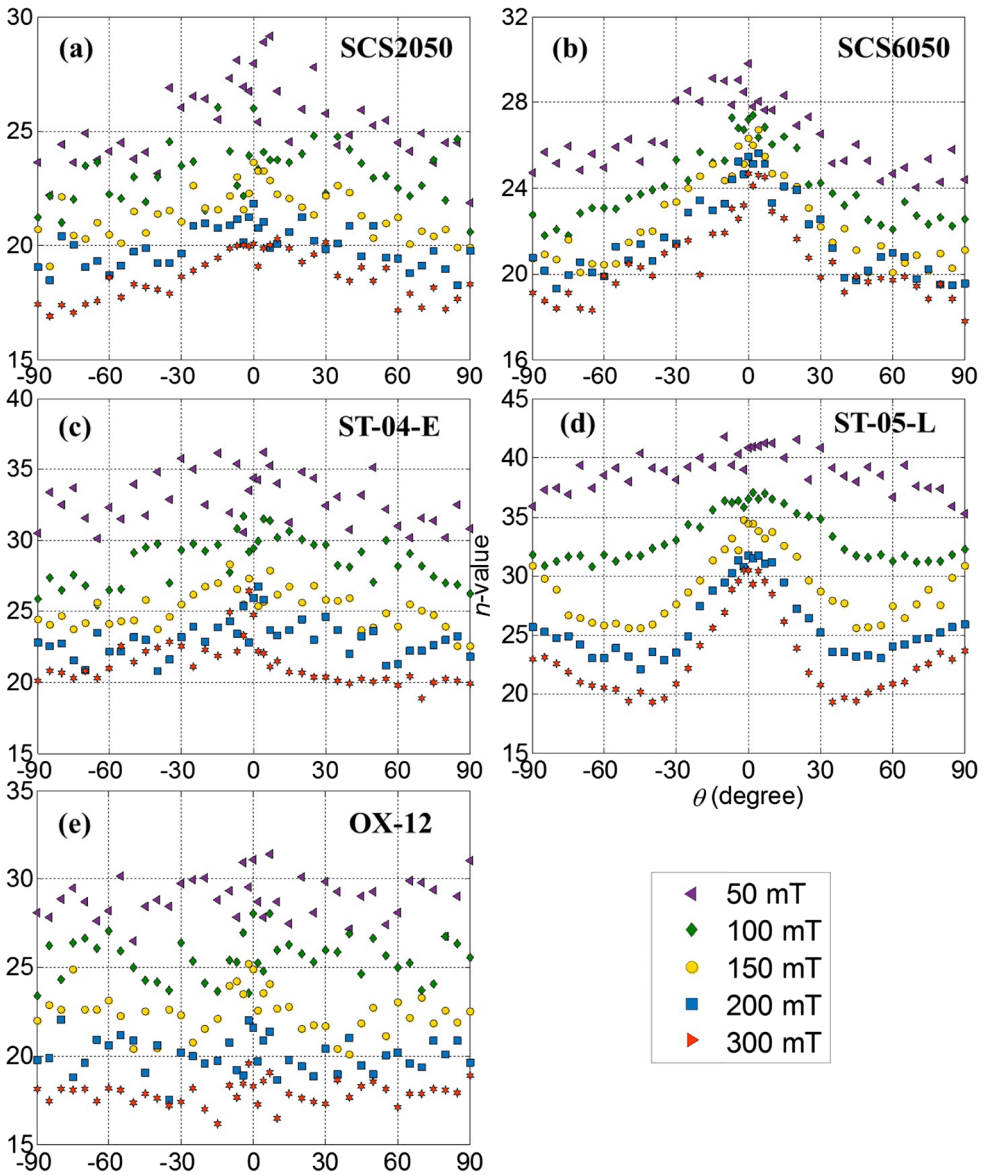

Fig. 3 (Colour online) Magnetic field-angular dependence of n-value characteristics in studied 2G HTS tapes. The definition of x-axis, the angle (θ) between the external field and the tape surface, is kept the same as in Fig. 2

It can be seen clearly that in all five cases, the n-values were always correlated to the critical current of the measured tapes, a fact that has been observed in numerous experimental studies [19, 20]. In detail, since the SuperPower tapes (SCS 2050 and SCS 6050) have identical structure, they both showed similar n-values, which varied in the same range with respect to the increase of B from 50 to 300 mT. Moreover, minor but noticeable angular dependence could be seen when a magnetic field existed, as shown in Fig. 3a, b.

Among all measured tapes, the two samples from SHSC exhibited the highest self-field n-values, and therefore the highest self-field critical current density, as can be seen from Fig. 3c, d and Table 1. However, their n-values fell relatively fast under the external field: with B climbing to 300 mT, their n-values declined to a level similar to that of the other three samples. Regarding angular dependence, the two tapes performed quite differently. Specifically, the curves of n-values of ST-04-E remained flat even under magnetic field $B = 300$ mT, while ST-05-L showed obvious anisotropy with all magnitudes of the applied magnetic field.

In addition, the n-values of Russian sample SO-12 decreased from 30 to 17 during our field-dependence test, but stayed unaffected when the relative angle between external B and the tape surface was adjusted. This observation is in good agreement with its critical current characteristics, which proves again that SO-12 is the best choice out of the five studied samples to work inside a rotating magnetic field.

5 Conclusion

In this paper, we have presented a thorough study about magnetic field-angular dependence of 2G HTS coated conductors. The features of the critical current of five commercial YBCO tapes manufactured by three companies were measured sequentially from $-90°$ to $+90°$, with an external magnetic field from 50 up to 300 mT. It was found that the angular dependence of the critical current increased with the rise of the magnitude of the magnetic field. After then, the $J_c(B, \theta)$ characteristics obtained from the experiment were accurately fitted using a general model we developed before, whose applicability and universality were proved by this work. Moreover, the magneto-angular dependence of n-values was calculated and analysed, showing that for the studied tapes n-values are directly correlated with their critical current profiles. Our results may be helpful to the design of HTS applications which require superconducting wires operating inside the external magnetic field.

Acknowledgements Xiuchang Zhang acknowledges a grant from the China Scholarship Council (No. 201408060080).

References

1. Sundaram, A., Zhang, Y., Knoll, A., Abraimov, D., Brownsey, P., Kasahara, M., et al.: 2G HTS wires made on 30 μm thick Hastelloy substrate. Supercond. Sci. Technol. **29**, 104007 (2016)
2. Nakasaki, R., Brownsey, P., Sundaram, A., Zhang, Y., Hazelton, D., Sakamoto, H., et al.: Progress of 2G HTS wire development at superpower. In: Proc. Appl. Supercond. Conf. (2016)
3. Geng, J., Shen, B., Li, C., Zhang, H., Matsuda, K., Li, J., et al.: Voltage-ampere characteristics of YBCO coated conductor under inhomogeneous oscillating magnetic field. Appl. Phys. Lett. **108**, 262601 (2016)
4. Ma, J., Zhu, J., Wu, W., Sheng, J., Yao, Z., Li, Z., et al.: Axial tension and overcurrent study on a type of mass-producible joint for ReBCO coated conductors. IEEE Trans. Appl. Supercond. **26**, 1–5 (2016)
5. Zhang, X., Ruiz, H., Geng, J., Coombs, T.: Optimal location and minimum number of superconducting fault current limiters for the protection of power grids. Int. J. Electr. Power Energy Syst. **87**, 136–143 (2017)
6. Zhang, X., Ruiz, H.S., Geng, J., Shen, B., Fu, L., Zhang, H., et al.: Power flow analysis and optimal locations of resistive type superconducting fault current limiters. SpringerPlus **5**, 1972 (2016)
7. Vojenčiak, M., Šouc, J., Ceballos, J., Gömöry, F., Klinčok, B., Pardo, E., et al.: Study of ac loss in Bi-2223/Ag tape under the simultaneous action of ac transport current and ac magnetic field shifted in phase. Supercond. Sci. Technol. **19**, 397 (2006)
8. Rostila, L., Lehtonen, J., Mikkonen, R., Šouc, J., Seiler, E., Melíšek, T., et al.: How to determine critical current density in YBCO tapes from voltage–current measurements at low magnetic fields. Supercond. Sci. Technol. **20**, 1097 (2007)
9. Pardo, E., Vojenčiak, M., Gömöry, F., Šouc, J.: Low-magnetic-field dependence and anisotropy of the critical current density in coated conductors. Supercond. Sci. Technol. **24**, 065007 (2011)
10. Zhang, X., Zhong, Z., Ruiz, H., Geng, J., Coombs, T.: General approach for the determination of the magneto-angular dependence of the critical current of YBCO coated conductors. Supercond. Sci. Technol. **30**, 025010 (2017)
11. SuperPower 2G HTS Wire. Available: http://www.superpower-inc.com/system/files/SP_HTS+Energy_2014_v1.pdf. Accessed 20 Mar 2018
12. Shanghai Superconductor Technology Co. Ltd. 2G HTS strip. Available: http://www.shsctec.com/Pages/SpecialProductList.aspx?ID=64&cl=en. Accessed 20 Mar 2018
13. SuperOx 2G HTS Wire. Available: http://www.superox.ru/products/0001.pdf. Accessed 20 Mar 2018
14. Blatter, G., Feigel'man, M.V., Geshkenbein, V.B., Larkin, A.I., Vinokur, V.M.: Vortices in high-temperature superconductors. Rev. Mod. Phys. **66**, 1125 (1994)
15. Tachiki, M., Takahashi, S.: Strong vortex pinning intrinsic in high-T c oxide superconductors. Solid State Commun. **70**, 291–295 (1989)

16. Kim, Y., Hempstead, C., Strnad, A.: Critical persistent currents in hard superconductors. Phys. Rev. Lett. **9**, 306 (1962)
17. Harshman, D., Schneemeyer, L., Waszczak, J., Aeppli, G., Cava, R., Batlogg, B., et al.: Magnetic penetration depth in single-crystal Y Ba 2 Cu 3 O 7 − δ. Phys. Rev. B **39**, 851 (1989)
18. Grilli, F., Sirois, F., Zermeno, V.M., Vojenciak, M.: Self-consistent modeling of the of HTS devices: how accurate do models really need to be? IEEE Trans. Appl. Supercond. **24**, 1–8 (2014)
19. Willis, J.O., Coulter, J.Y., Rupich, M.W.: N-value analysis of position-dependent property variability in long-length coated conductors. IEEE Trans. Appl. Supercond. **21**, 2988–2991 (2011)
20. Hong, Z., Hong, W., Cong-Xin, R., Guo-Liang, C.: The anisotropy of the current-carrying characteristics of YBCO film fabricated by magnetron sputtering. Supercond. Sci. Technol. **7**, 359 (1994)